

Tuning quadratic nonlinear photonic crystal fibers for zero group-velocity mismatch

Morten Bache, Hanne Nielsen, Jesper Lægsgaard, and Ole Bang

COM-DTU, Technical University of Denmark, Building 345v, DK-2800 Lyngby, Denmark

Received November 29, 2005; revised March 16, 2006; accepted March 27, 2006; posted March 28, 2006 (Doc. ID 66350)

We consider an index-guiding silica photonic crystal fiber with a triangular hole pattern and a periodically poled quadratic nonlinearity. By tuning the pitch and the relative hole size, second-harmonic generation with zero group-velocity mismatch is found for any fundamental wavelength above 780 nm. The nonlinear strength is optimized when the fundamental has maximum confinement in the core. The conversion bandwidth allows for femtosecond-pulse conversion, and 4%–180% $W^{-1} \text{cm}^{-2}$ relative efficiencies were found.

© 2006 Optical Society of America

OCIS codes: 060.2280, 060.2400, 060.4370, 320.7110.

Second-harmonic generation (SHG) is widely used for efficient wavelength conversion devices for extending the spectral range of laser sources and all-optical wavelength multiplexing. Efficient conversion from the fundamental to the second-harmonic (SH) occurs only close to phase matching. To lowest order it is typically achieved through a quasi-phase-matching (QPM) technique,¹ so the group-velocity mismatch (GVM) limits the device length and bandwidth for pulsed SHG. For fiber SHG, zero GVM for restricted wavelengths was predicted to be achievable by changing the core radius² and by using mode-matching.³ In bulk media zero GVM was found for restricted wavelengths by spectrally noncritical phase matching⁴ and by combining noncollinear QPM with a pulse-front tilt.⁵

Here we investigate efficient pulsed SHG in a silica index-guiding photonic crystal fiber (PCF) with a triangular air-hole pattern and a single-rod core defect; see the inset in Fig. 1(a). The PCF design parameters are the pitch Λ and the relative hole size $D=d/\Lambda$. We assume a quadratic nonlinearity from thermal poling of the PCF.⁶

As is shown below, the SHG conversion efficiency, defined as the output SH power relative to the input fundamental power P_1 , is $\eta \propto P_1 \rho^2 l_F^2 \text{sinc}^2(\Delta\beta l_F/2)$. Efficient SHG can be achieved by increasing P_1 , as well as by having a large nonlinear material response and a strong modal overlap, which both are included in the ρ parameter. The coherence length l_{coh} of the mode phase mismatch $\Delta\beta$ to the lowest order gives the range (typically micrometers) over which power is exchanged efficiently to the SH, after which the power flow reverses. A QPM grating can compensate for this. Converting ultrashort transform-limited Gaussian pulses of duration τ requires a large SHG bandwidth $\Delta\lambda$, because $\Delta\lambda = 2 \ln(2) \lambda_1^2 / (\pi c \tau)$. Neglecting the weak frequency dependence on ρ , $\Delta\lambda$ is determined by the width of $\text{sinc}^2(\Delta\beta l_F/2)$. Thus taking a small fiber length l_F gives a large $\Delta\lambda$ but also a poor efficiency because $\eta \propto l_F^2$. We will instead minimize $\Delta\beta$, whose first-order contribution is the GVM: thus zero GVM gives larger bandwidths. Also, GVM implies a temporal walk-off length l_W between the modes, so we are forced to take $l_F \leq l_W$. When GVM is

zero, $l_W \rightarrow \infty$, and l_F can be taken longer, thereby increasing η dramatically.

PCFs are interesting candidates for efficient fiber SHG because of their flexibility concerning dispersion design⁷ and maximizing the nonlinear strength.⁸ A scalar analysis of SHG in PCFs found large bandwidths and strong modal overlaps for selected parameters.⁹ Instead, we perform a detailed vectorial analysis over a continuous parameter space and show zero GVM for any fundamental wavelength $\lambda_1 > 780$ nm by merely adjusting the pitch and the relative hole size. Such a degree of tunability has never been demonstrated before to our knowledge and has great promise compared with the previous methods of Refs. 3–5.

We describe a fiber mode by an effective index $n = c/v_{\text{ph}}$, where c is the speed of light, $v_{\text{ph}} = \omega/\beta$ is the mode phase velocity, and β is the mode propagation constant. We describe the lowest-order phase mismatch of the interaction by the index mismatch $\Delta n = n(\omega_1) - n(\omega_2) = c[1/v_{\text{ph}}(\omega_1) - 1/v_{\text{ph}}(\omega_2)] = c(\beta_1/\omega_1 - \beta_2/\omega_2)$ between ω_1 (fundamental mode) and $\omega_2 = 2\omega_1$ (SH mode). Thus Δn describes a mismatch in the phase velocities. The relation to the lowest-order phase mismatch $\Delta\beta \equiv 2\beta_1 - \beta_2$ is $\Delta\beta = 4\pi\Delta n/\lambda_1$. The group velocity of the mode is instead defined as $1/v_g = \partial_\omega\beta = \partial_\omega$

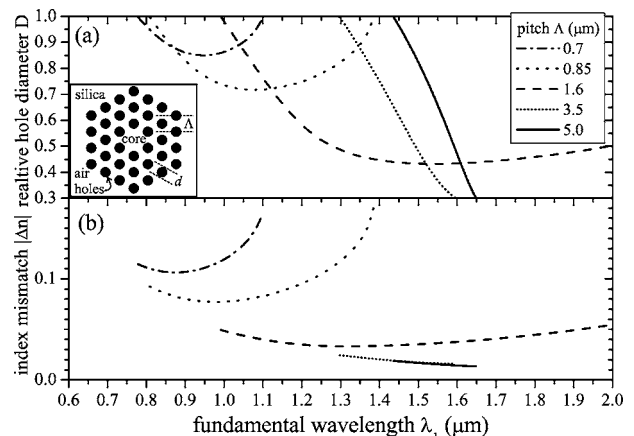


Fig. 1. (a) Zero-GVM contours in (λ_1, D) space; (b) $|\Delta n|$ along these contours. Λ is fixed at selected values. Inset, PCF with pitch Λ and air-hole diameter d .

$\equiv \partial/\partial\omega$, giving a GVM (walk-off) parameter $d_{12} = [1/v_g(\omega_1) - 1/v_g(\omega_2)]$.

We calculated the fiber modes with the MIT Photonic-Bands (MPB) package.¹⁰ Each unit cell contained $n_C^2 = 32^2$ grid points, and the super cell contained $n_{SC}^2 = 5^2$ unit cells. The fundamental mode frequency and group velocity were first calculated, followed by iterations of the SH until $|\omega_2 - 2\omega_1| < 10^{-8}$. Material dispersion, parameterized by the silica Sellmeier equation,¹¹ was then included by using a perturbative technique,¹² whose advantage is that many different Λ values can be calculated perturbatively from the MPB data (where Λ is unity.)

The calculated GVM parameter d_{12} is shown in Fig. 1(a) as a zero-GVM contour ($d_{12}=0$) for $0.6 \leq \lambda_1 \leq 2.0 \mu\text{m}$ and $0.3 \leq D \leq 1$, while keeping the pitch Λ fixed. The examples show that the design parameters can be tuned over a continuous range to achieve zero GVM for any $\lambda_1 > 0.78 \mu\text{m}$. In Fig. 1(b) we show that the corresponding index mismatch $|\Delta n|$ is never zero. This is a general trend, even with nonzero GVM, so a QPM method is needed to achieve lowest-order phase matching. In Fig. 1(b) we also note that for $\Lambda = 0.70, 0.85, 1.6 \mu\text{m}$ a minimum in $|\Delta n|$ appears around $\lambda_1 \approx \Lambda$. We confirmed that the core diameter $d_c \approx \Lambda(2 - D)$ relative to λ_1 is maximum there. Thus, when λ_1 increases beyond this point, d_c/λ_1 shrinks; so the fundamental is less confined in the core. Since the SH stays well confined (because $\lambda_2 = \lambda_1/2$), an increase in $|\Delta n|$ follows.

Let us focus on the telecommunications, Nd:YAG, and Ti:sapphire operating wavelengths ($\lambda_1 = 1.55, 1.06$, and $0.80 \mu\text{m}$, respectively.) In Fig. 2(a) we then show the D value necessary to get zero GVM as Λ is changed. For $\lambda_1 = 0.80 \mu\text{m}$, zero GVM requires $D \geq 0.96$. For such large D values, deviations from the ideal circular holes must be expected, which might influence the results presented here. However, to our knowledge this is the first time that zero GVM has been demonstrated for SHG in any material for $\lambda_1 = 0.80 \mu\text{m}$. Instead, for both $\lambda_1 = 1.06 \mu\text{m}$ and $\lambda_1 = 1.55 \mu\text{m}$ the D values are in a range where the ideal round holes should be preserved. In Fig. 2(b) we calculate the SHG bandwidth $\Delta\lambda$ of the $\text{sinc}^2(\Delta\beta l_F/2)$ term by expanding^{1,5} $\Delta\beta(\lambda_1 + \Delta\lambda) = \sum_m (m!)^{-1} \Delta\lambda^m \partial_\lambda^m \Delta\beta$ and assuming that a QPM grating compensates for the $m=0$ term. Since $d_{12}=0$, the second-order dispersion dominates, yielding very large bandwidths. The bandwidth scales favorably as $\Delta\lambda \propto l_F^{-1/2}$ because $d_{12}=0$ (instead of $\Delta\lambda \propto l_F^{-1}$ for $d_{12} \neq 0$); so l_F can be larger without losing too much bandwidth. The large peaks in Fig. 2(b) can be explained from Fig. 1(a): a minimum in the zero-GVM contour implies that the $m=2$ term vanishes, giving very large $\Delta\lambda$. Such a minimum occurs at $\lambda_1 = 1.55 \mu\text{m}$ (for $\Lambda = 1.6 \mu\text{m}$) and at $\lambda_1 = 1.06 \mu\text{m}$ (for $\Lambda = 0.85 \mu\text{m}$). Finally, Fig. 2(c) shows the QPM period $l_{\text{QPM}} = 2|l_{\text{coh}}| = 2\pi/|\Delta\beta(\lambda_1)| = \lambda_1/(2|\Delta n|)$ necessary to achieve lowest-order phase matching. Such values can be reached by using periodic poling: either by writing the periodic pattern by using photolithography on the electrode placed on the flat part

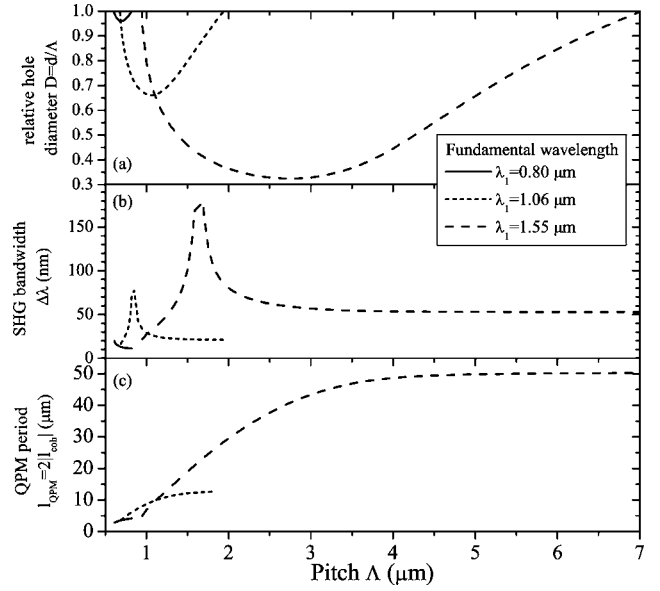


Fig. 2. (a) Zero-GVM contours in (Λ, D) space, fixing λ_1 ; (b) $\Delta\lambda$ for $l_F = 10$ cm and (c) l_{QPM} along these contours.

of a D-shaped fiber² or by using laser ablation on an electrode deposited in the fiber.¹³

Next we used the reductive perturbation method¹⁴ to derive the dimensionless nonlinear equations for SHG:

$$(\partial_z - i\tilde{D}_1\partial_t^2)u_1 = i\sigma u_1 u_2 e^{-i\Delta\beta z l_F}, \quad (1)$$

$$(\partial_z - \tilde{d}_{12}\partial_t - i\tilde{D}_2\partial_t^2)u_2 = i\sigma u_1^2/2e^{i\Delta\beta z l_F}. \quad (2)$$

In the derivation we have assumed a weak nonlinearity (uniform over the silica part of the PCF), so we may take $\mathbf{E}_j(\mathbf{r}) = A_j(z, t)\mathbf{e}_j(\mathbf{x})e^{i(\beta_j z - \omega_j t)} + \text{c.c.}$, where $\mathbf{x} = (x, y)$. We also assume weak transverse variations in the refractive index; so $\nabla \times (\nabla \times \mathbf{E}) = -\nabla^2 \mathbf{E}$. The retarded coordinate z is in the frame of reference traveling with velocity $v_g(\omega_1)$ and is normalized to l_F , while t is normalized to the input pulse length τ , $\tilde{d}_{12} = d_{12}l_F/\tau$, and $\tilde{D}_j = l_F/(2\tau^2)\partial_\omega^2 \beta_j$. We have defined $A_j(z, t) = u_j(z, t)(\Lambda^2 l_F / N_j n_j a_j c \tau)^{1/2}$, so $N_j(z) = \int dt |u_j(z, t)|^2$ gives the photon number. The dimensionless nonlinear strength is $\sigma = \rho l_F (2\hbar\omega_1^2 \omega_2 / n_1^2 n_2 \epsilon_0 c^3 \tau)^{1/2}$, where

$$\rho = (a_1^2 a_2)^{-1/2} \left| \int d\mathbf{x} \tilde{\mathbf{e}}_1^*(\mathbf{x}) \cdot \tilde{\chi}^{(2)}(\mathbf{x}) \cdot \tilde{\mathbf{e}}_2(\mathbf{x}) \tilde{\mathbf{e}}_1^*(\mathbf{x}) \right| \quad (3)$$

includes material nonlinearity through the quadratic nonlinear tensor $\tilde{\chi}^{(2)}(\mathbf{x})$ as well as the spatial mode overlap, whose effect on σ we investigate below. $\tilde{\mathbf{e}}_j(\mathbf{x}) = \mathbf{e}_j(\mathbf{x})(\epsilon_0 \Lambda^2 l_F / 2\hbar\omega_j N_j)^{1/2}$ are the dimensionless transverse MPB modes, and $a_j = \int d\mathbf{x} |\tilde{\mathbf{e}}_j(\mathbf{x})|^2$ are the mode areas. The modes being vectorial, their overlap cannot be characterized by one overlap area, but ρ^2 is equivalent to the scalar expression² $d_{\text{eff}}^2/A_{\text{ovl}}$ (the effective nonlinearity squared relative to the effective overlap area). We assumed the $\tilde{\chi}^{(2)}$ tensor to have the nonzero elements $\tilde{\chi}_{jji}^{(2)} = \tilde{\chi}_{jij}^{(2)} = \tilde{\chi}_{ijj}^{(2)} = \tilde{\chi}_{iii}^{(2)}/3$, where i is the

main direction of the poling voltage, and j is either of the two remaining directions.¹⁵ We chose $\tilde{\chi}_{xxx}^{(2)} = 1$ pm/V, which is feasible by thermal poling of fibers.² The considered PCF has two degenerate solutions that are x and y polarized, respectively; so it will suffice to consider $i=x$.

Figure 3 shows the nonlinear strength σ for λ_1 and D fixed (note that these curves are not zero-GVM contours.) A $2/\pi$ reduction of $\tilde{\chi}^{(2)}$ is included because we assume lowest-order phase matching through a QPM grating.¹ We found the scaling $\sigma \propto D/\Lambda = d/\Lambda^2$, which is due to a smaller core when Λ is reduced, and better core confinement when D is increased. σ peaks when Λ takes values around the chosen fundamental wavelength λ_1 (similar to what Ref. 8 observed) and drops for $\Lambda < \lambda_1$ because the fundamental mode has maximum core confinement at the peak [Fig. 3, inset (2)]. It becomes more poorly confined when $\Lambda < \lambda_1$, while the SH stays better confined [cf. Fig. 3, inset (1)], resulting in a poor modal overlap. A similar effect gives the minimum in $|\Delta n|$ in Fig. 1(b). For large D , a decent fundamental mode confinement is observed even for $\Lambda < \lambda_1$ [compare Fig. 3 inset (3) with inset (1)], giving a shift in the peak toward smaller Λ . σ also increases when λ_1 is reduced, because if d and Λ are fixed, the light is better confined for smaller λ . Table 1 shows data for selected designs of SHG with zero GVM. We confirmed that the fundamental is single mode for all three designs by using the criterion¹⁶ $\lambda_1/\Lambda > 2.80(D-0.406)^{0.89}$. For the $1.55 \mu\text{m}$ design the SH is also single mode. The SHG efficiency

$$\eta = \sigma^2 \text{sinc}^2(\Delta\beta l_F/2) P_1^2 / 2\hbar\omega_1 \\ = P_1 \rho^2 l_F^2 \text{sinc}^2(\Delta\beta l_F/2) 2\omega_1^2 / n_1^2 n_2 \epsilon_0 c^3$$

is found by solving Eq. (2) (assuming an undepleted fundamental and neglecting temporal dispersion). $\Delta\beta$ is here evaluated from the fundamental pulse bandwidth and the calculated dispersion. Very large relative efficiencies $\eta_r \equiv \eta/P_1 l_F^2$ are found. Last, the bandwidths give a limit τ_{lim} of a transform-limited pulse that can be converted, which is in the femtosecond

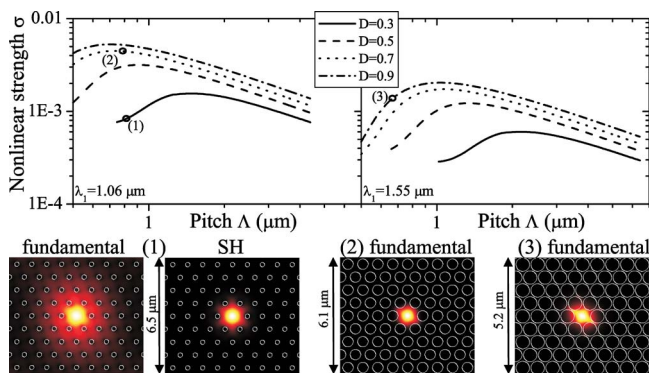


Fig. 3. (Color online) Double-log plots of σ versus Λ . Insets (1)–(3), selected mode energy distributions. $l_F = 10$ cm, $\tau = 1$ ps, $n_{\text{SC}} = 9$.

Table 1. Selected designs for SHG with zero GVM^a

λ_1 μm	Λ μm	D μm	$\Delta\lambda$ nm	τ_{lim} fs	l_{QPM} μm	σ 10^{-3}	η_r $\% \text{W}^{-1} \text{cm}^{-2}$
0.80	0.70	0.96	13	73	4.3	10.3	183.6
1.06	0.85	0.72	77	21	7.7	4.4	42.3
1.55	1.60	0.43	170	21	29.1	1.0	3.71

^a $l_F = 10$ cm, $\tau = 1$ ps, $\tilde{\chi}_{xxx}^{(2)} = 1$ pm/V.

range. Thus ultrashort pulse conversion is feasible.

To conclude, by tuning the pitch and relative hole size of an index-guiding silica PCF, SHG with zero GVM could be achieved for any $\lambda_1 > 780$ nm. The method holds great promise owing to its tunability and simplicity, and conversion bandwidths suitable for femtosecond pulse conversion were found. The SHG nonlinear strength was optimized when the fundamental was maximally confined, and it was inversely proportional to the pitch and proportional to the relative hole size. We found up to $180\% \text{W}^{-1} \text{cm}^{-2}$ relative conversion efficiencies.

M. Bache acknowledges support from The Danish Natural Science Research Council (FNU, grant 21-04-0506). M. Bache's e-mail address is bache@com.dtu.dk.

References

1. M. M. Fejer, G. A. Magel, D. H. Jundt, and R. L. Byer, *IEEE J. Quantum Electron.* **28**, 2631 (1992).
2. P. G. Kazansky and V. Pruneri, *J. Opt. Soc. Am. B* **14**, 3170 (1997).
3. A. Arraf and C. M. de Sterke, *IEEE J. Quantum Electron.* **34**, 660 (1998).
4. N. E. Yu, J. H. Ro, M. Cha, S. Kurimura, and T. Taira, *Opt. Lett.* **47**, 1046 (2002).
5. S. Ashihara, T. Shimura, and K. Kuroda, *J. Opt. Soc. Am. B* **20**, 853 (2003).
6. D. Faccio, A. Busacca, W. Belardi, V. Pruneri, P. Kazansky, T. Monro, D. Richardson, B. Grappe, M. Cooper, and C. Pannell, *Electron. Lett.* **37**, 107 (2001).
7. A. Ferrando, E. Silvestre, P. Andrés, J. J. Miret, and M. V. Andrés, *Opt. Express* **9**, 687 (2000).
8. J. Lægsgaard and A. Bjarklev, *J. Opt. A* **6**, 1 (2004).
9. T. M. Monro, V. Pruneri, N. G. R. Broderick, D. Faccio, P. G. Kazansky, and D. J. Richardson, *IEEE Photon. Technol. Lett.* **13**, 981 (2001).
10. S. Johnson and J. Joannopoulos, *Opt. Express* **8**, 173 (2001).
11. J. W. Fleming, *Electron. Lett.* **14**, 326 (1978).
12. J. Lægsgaard, A. Bjarklev, and S. Libori, *J. Opt. Soc. Am. B* **20**, 443 (2003).
13. N. Myrén, M. Fokine, O. Tarasenko, L.-E. Nilsson, H. Olsson, and W. Margulis, *J. Opt. Soc. Am. B* **21**, 2085 (2004).
14. Y. Kodama and A. Hasegawa, *IEEE J. Quantum Electron.* **QE-23**, 510 (1987).
15. S. Kielich, *IEEE J. Quantum Electron.* **5**, 562 (1969).
16. B. T. Kuhlmey, R. C. McPhedran, and C. M. de Sterke, *Opt. Lett.* **27**, 1684 (2002).